# Optimizing Interface Conductivity in Electronics

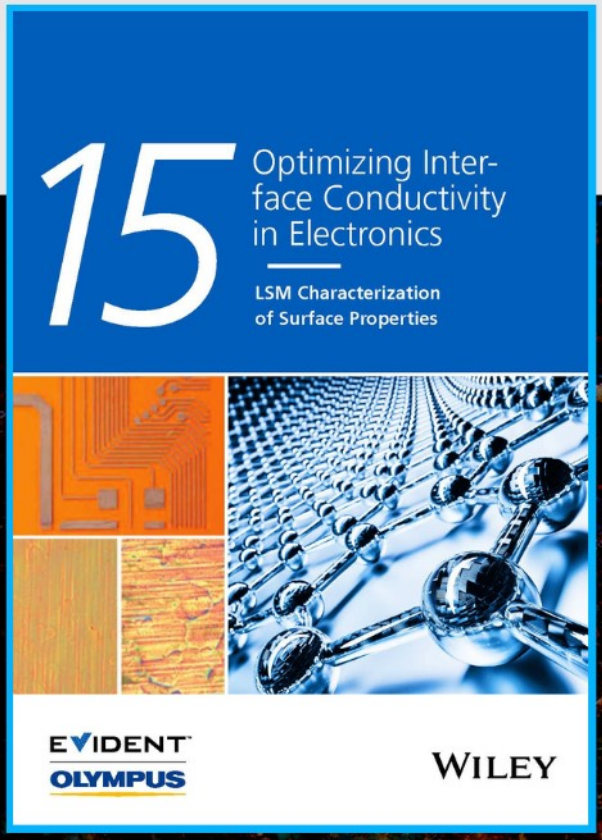


**The latest eBook from Advanced Optical Metrology. Download for free.**

Surface roughness is a key parameter for judging the performance of a given material's surface quality for its electronic application. A powerful tool to measure surface roughness is 3D laser scanning confocal microscopy (LSM), which will allow you to assess roughness and compare production and finishing methods, and improve these methods based on mathematical models.

Focus on creating high-conductivity electronic devices with minimal power loss using laser scanning microscopy is an effective tool to discern a variety of roughness parameters.

EVIDENT
OLYMPUS

WILEY

ADVANCED FUNCTIONAL MATERIALS
www.afm-journal.de

# Electric Current Aligning Component Units during Graphene Fiber Joule Heating

*Yi Cheng, Guang Cui, Changhao Liu, Zhetong Liu, Longge Yan, Bingyao Liu, Hao Yuan, Pengcheng Shi, Jun Jiang, Kewen Huang, Kun Wang, Shuting Cheng, Junliang Li, Peng Gao, Xinfang Zhang,* Yue Qi,* and Zhongfan Liu**

**Joule heating is featured with an extremely high rising rate of temperature with hundreds of kelvin per second, which has shown superiorities of high efficiency and energy conservation in graphene fabrication. Herein, we design a dynamic joule heating system for continuous synthesis of graphene fibers with ultrashort high-temperature (≈2000 °C), treating time (≈20 min), and low electric energy consumption (≈2000 kJ $m^{-1}$). During the joule heating fabrication, the current flowing through the fibers can manipulate the configuration of graphene sheets, the basic component units of fiber, and induce their alignment. Theoretical simulations reveal that graphene sheets tend to rotate towards the current direction under the current induced electric field for the highest stability with the lowest electric free energy and zero rotation torque. Therefore, the electrical and mechanical performances of as-fabricated graphene fibers can be further improved in comparison with thermally annealed graphene fibers without applying current.**

## 1. Introduction

Joule heating is emerged as an advanced method for the efficient fabrication of thermodynamically stable or metastable materials, such as carbon materials,[1–6] bulk ceramics,[7] transition metal dichalcogenide,[8] and high-entropy-alloy nanoparticles.[9] During joule heating, the temperature can reach about 3000 K in few seconds when current flows through the conductors,[7,10] which overcomes the dilemma of traditional heating types requiring bulky-sized furnace with low temperature raising rate (<100 K $min^{-1}$).[11,12]

Electric current field is widely utilized to control the microstructure of materials composed of independent units by modulating their kinetic barrier and free energy. Under this manipulation, the component units can change their conformation and move along the lowest free energy route.[13–16] For example, it has been reported that under the current induced electric field, the fragmented lamellar cementite inclusions in ferritic-pearlitic steel tended to align their configurations parallel to the current direction, along which the inclusions have the lowest free energy.[17]

Graphene fiber, as a new member of carbonaceous fibers assembled by graphene sheets as component units, is deemed to exhibit remarkable performances in 1D by inheriting the superior electrical, mechanical, and thermal properties of intrinsic graphene.[18–22] Currently, the prevailing strategy for

Y. Cheng, Dr. G. Cui, Z. T. Liu, B. Y. Liu, H. Yuan, K. W. Huang, K. Wang, Dr. Y. Qi, Prof. Z. F. Liu
Center for Nanochemistry
Beijing Science and Engineering Center for Nanocarbons
Beijing National Laboratory for Molecular Sciences
College of Chemistry and Molecular Engineering
Peking University
Beijing 100871, P. R. China
E-mail: qiyue-cnc@pku.edu.cn; zfliu@pku.edu.cn

Y. Cheng, Dr. G. Cui, Z. T. Liu, B. Y. Liu, H. Yuan, P. C. Shi, J. Jiang, K. W. Huang, K. Wang, S. T. Cheng, J. L. Li, Prof. P. Gao, Dr. Y. Qi, Prof. Z. F. Liu
Beijing Graphene Institute (BGI)
Beijing 100095, P. R. China

The ORCID identification number(s) for the author(s) of this article can be found under https://doi.org/10.1002/adfm.202103493.

DOI: 10.1002/adfm.202103493

C. H. Liu, L. G. Yan, Prof. X. F. Zhang
State Key Laboratory of Advanced Metallurgy
School of Metallurgical and Ecological Engineering
University of Science and Technology Beijing
Beijing 100083, P. R. China
E-mail: xfzhang@ustb.edu.cn

Z. T. Liu, B. Y. Liu, Prof. P. Gao
Academy for Advanced Interdisciplinary Studies
Peking University
Beijing 100871, P. R. China

Z. T. Liu, B. Y. Liu, Prof. P. Gao
Electron Microscopy Laboratory and International Center for Quantum Materials
School of Physics
Peking University
Beijing 100871, P. R. China

J. Jiang, S. T. Cheng
State Key Laboratory of Heavy Oil Processing
College of Science
China University of Petroleum
Beijing 102249, P. R. China

 

graphene fiber synthesis is graphene oxide (GO) wet spinning, followed with the GO fiber reduction to remove oxygen-containing functional groups and heal defects.[23–26] The reduction process can lead to several to dozens times improvement of electrical, mechanical, and thermal properties of fiber.[23,24,27–29] Thereinto, high-temperature thermal treatment is considered as one of the most effective approaches to reduce GO fibers, eliminate the non-carbon impurities, and improve the crystallinity of graphene fibers.[27,28,30–32] Nonetheless, this method always requires quite a long duration (>12 h) at high temperature (>2000 °C), which will cause the decrease in productivity and the increase in fabricating cost. In addition, the conformation order of graphene sheets in fibers is a significant parameter for fiber performances. The higher sheet orientation can reduce the structure disorder and improve the compactness of graphene fibers, leading to better electrical and mechanical properties.[26,27,29,33] Therefore, it is highly desirable to develop an effective strategy to synthesize graphene fibers, while improving the conformation order of the inner graphene sheets.

In this work, the joule heating method was applied to the fabrication of graphene fibers and the dynamic design was innovatively integrated to achieve the continuous production. The joule heating can convert defective graphene oxide (GO) fibers into highly crystalline graphene fibers with an ultrashort high-temperature treating time (20 min at ≈2000 °C) and a low energy consumption (≈2000 kJ $m^{-1}$). Moreover, the current-induced electric field was first utilized to orientate the graphene sheets, the basic component units of fiber, parallel to the current direction and increase their conformation order. The increase of the sheet conformation order can further benefit the improvements the fiber properties. Compared with conventional thermally annealed graphene fibers (TGFs) without current applying, the joule-heated graphene fibers (JGFs) exhibited a higher Herman's orientation factor (0.73, 16% increase), resulting in superior electrical conductivity (≈$5.9 \times 10^5$ S $m^{-1}$, 11% increase) and tensile strength (≈1.07 GPa, 20% increase). This scalable method paves an innovative way for the quick and continuous production of graphene fibers with high efficiency and massive productivity, which will facilitate their real applications in power cables, electromagnetic shielding, and wearable electronics, etc. In addition, the current-inducing effect during this process can be applied into the conformation manipulating of component units in assembled materials, which has a promising potential in further improving their macroscopic performances.

## 2. Results and Discussion

The home-made dynamic joule heating (DJH) equipment for the continuous fabrication of graphene fibers consists of four major parts, including joule heating module, roll-to-roll apparatus, and vacuum and gas supplying systems (**Figure 1**a and Figure S1, Supporting Information). During DJH process, a bundle of chemically reduced GO (rGO) fibers coiled on two winding rollers moved through the joule heating zone with a programmed velocity (see Experimental Section for more details). Meanwhile, an infrared camera was utilized to monitor the temperature of JGFs. When the input current flowed through graphene fibers, temperature of the fibers between two electrode pulleys can raise to a steady value within few seconds due to the joule heating effect (Figure S2 and Movie S1, Supporting Information). The as-fabricated JGFs exhibit uniform gray contrast and high flexibility after the joule heating

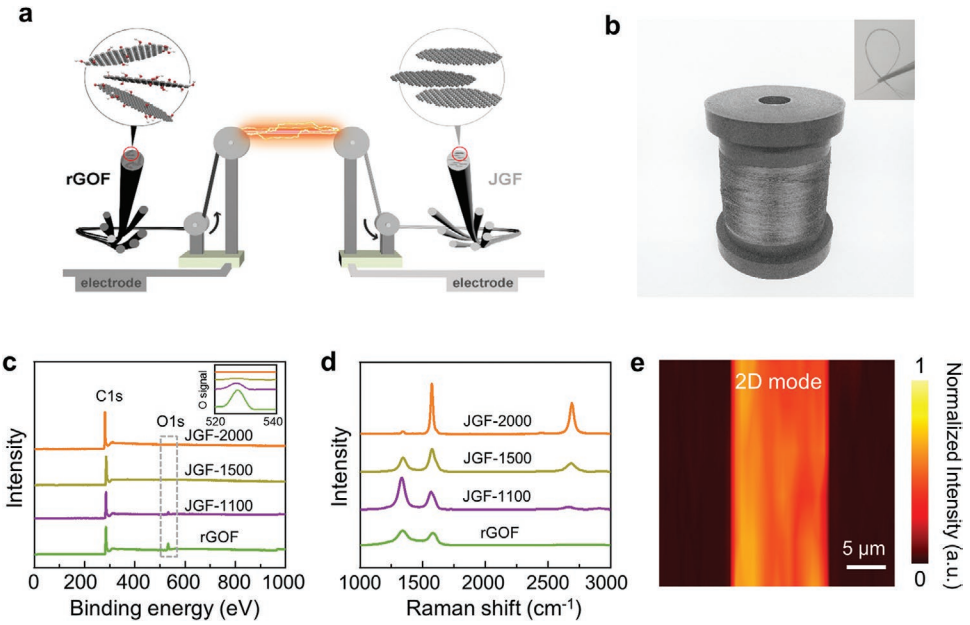


**Figure 1.** Graphene fibers fabricated by DJH method. a) Schematic of the DJH system. rGOFs coiled on the supplying roller continuously moved through the joule heating zone to the receiving roller. b) A reel of 100-filament JGFs. The inset shows the flexibility of as-fabricated JGFs. c) XPS spectra of rGOFs, JGFs annealed at 1100 °C for 10 min (denoted as JGFs-1100), JGFs treated at 1500 and 2000 °C for 10 min after 10-min treatment at 1100 °C (denoted as JGFs-1500 and JGFs-2000, respectively). The inset is the zoomed-in O 1s XPS spectra corresponding to the region in the gray dashed box. d) Raman spectra of rGOFs and JGFs experiencing the same treatment as that in (c). e) 2D-mode Raman intensity mapping of single JGF-2000.

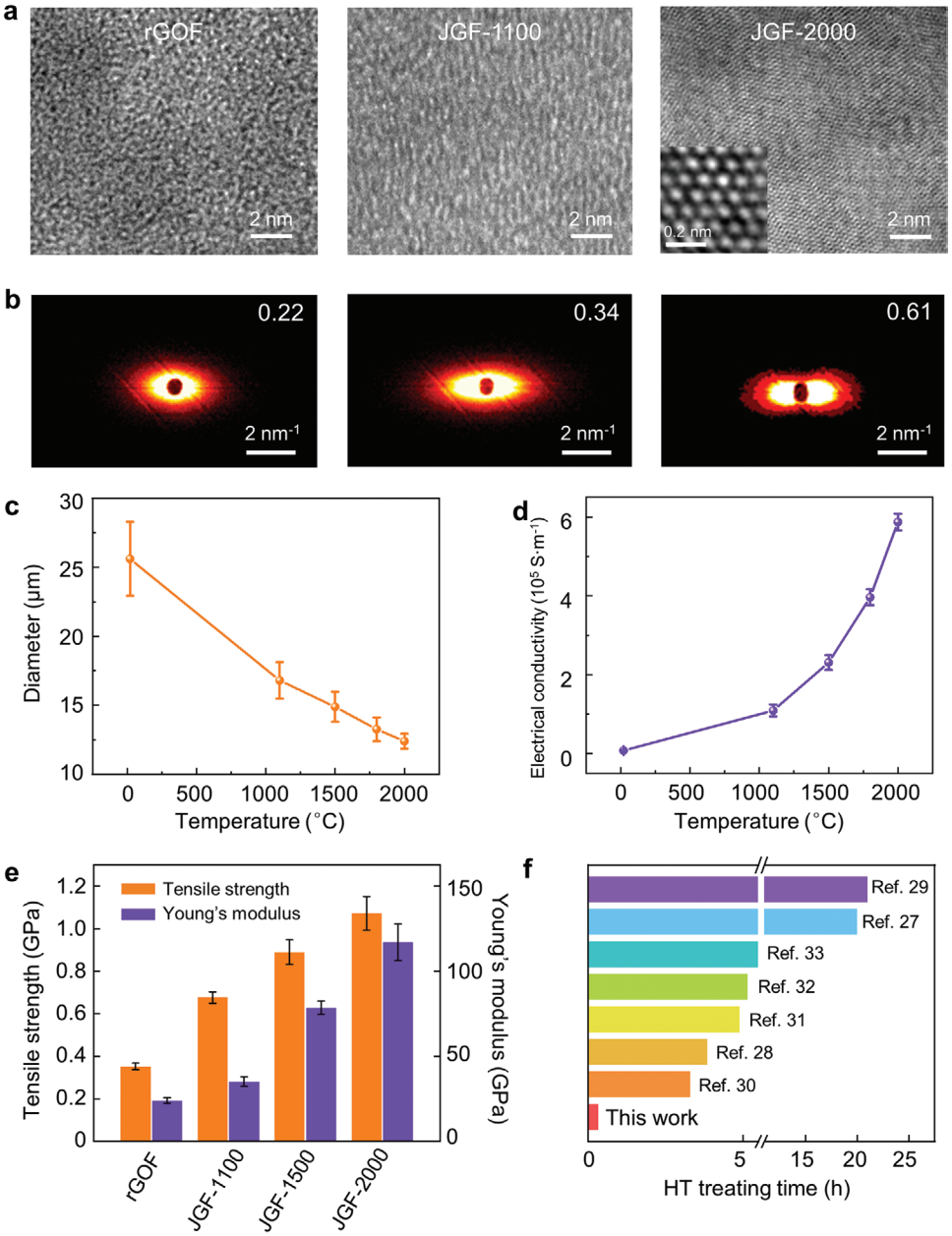


**Figure 2.** Temperature-dependent structures and properties of JGFs. a) HR-TEM images of rGOFs, JGFs-1100 and JGFs-2000. Inset is the atomic resolution image of JGFs-2000. b) Corresponding SAXS patterns of rGOFs, JGFs-1100, and JGFs-2000 in (a). c,d) Temperature-dependent diameter (c) and electrical conductivity (d) of JGFs. e) Temperature-dependent tensile strength and Young's modulus of JGFs. f) Comparison of high-temperature (HT) treating time between JGFs with previously reported thermally treated graphene fibers (Refs. [27–33]). Error bars represent the standard deviations from measurements of ten different fibers in (c–e) and 10 different positions of each fiber in (c,d).

treatment (Figure 1b and inset). The high temperature during DJH process can effectively remove the non-carbon impurities and enhance the fiber crystallinity. The impurity elimination was characterized by X-ray photoelectron spectroscopy (XPS), revealing that O 1s peak at ≈533 eV gradually decreases with temperature increase until finally disappearing at 2000 °C (Figure 1c and inset), consistent with the corresponding energy disperse spectroscopy (EDS) and thermogravimetric (TG) results (Figures S3 and S4, Supporting Information). In contrast to rGO fibers (rGOFs), the JGFs treated at 2000 °C (JGFs-2000) show a negligible D peak in the Raman spectra (Figure 1d), along with a uniform 2D peak intensity mapping (Figure 1e), indicating the high quality of the as-fabricated JGFs.

To analyze microstructure evolution of graphene fibers during DJH process, high-resolution transmission electron microscopy (HR-TEM) (**Figure 2**a) was employed, which reveals that the amorphous structure of rGOFs can be effectively converted into highly crystalline structure with regular Moiré patterns, as presented in JGFs-2000. Atomic resolution image in the inset of Figure 2a exhibits the well-arranged carbon atoms,

confirming the high quality of as-fabricated JGFs. Furthermore, corresponding small-angle X-ray scattering (SAXS) patterns show stronger equatorial scattering patterns with the orientation degree increasing from 0.22 to 0.61 (Figure 2b), which indicates a gradual increase of sheet alignment during the DJH process. Microstructure can contribute a vital part to the macroscopic performances. Benefitting from the improvement of the crystalline quality and sheet alignment with the temperature ascending, the electrical and mechanical properties of JGFs increase synchronously, accompanied with a diameter shrinkage (Figure 2c–e and Figures S5 and S6, Supporting Information). Specifically, JGFs-2000 can achieve a superior and uniform electrical conductivity of $(5.9 \pm 0.2) \times 10^5$ S m$^{-1}$, surpassing the majority of polyacrylonitrile (PAN)- or pitch-based carbon fibers.[34–36] The uniformity of JGFs was further confirmed by the uniform distribution of electro-thermal temperature (Figure S7, Supporting Information). The tensile strength and Young's modulus of JGFs-2000 can reach to a value of $1.07 \pm 0.08$ GPa and $116 \pm 10$ GPa, respectively. Compared with conventional thermal treatments, the total high-temperature duration time of graphene fibers during DJH process is as low as 20 min, which is more than one order of magnitude shorter than conventional thermal treating time, as summarized in Figure 2f.[27–33]

In addition to healing the defects and increasing the graphene crystallinity through high-temperature treatment, joule heating can also increase the conformation order of graphene sheet component units in fibers due to the existence of the current-induced electric field. To clarify the effects of the electric current flowing through fibers, graphene fiber counterparts obtained by the conventional thermally annealing method, called TGFs for short, were included for comparison, which were treated with the same temperature and time (see Experimental Section for more details). The crystallinity and purity of TGFs were characterized by the Raman and XPS (Figure S8, Supporting Information), showing negligible difference compared with JGFs. The orientation order of graphene sheets in JGFs was significantly improved compared with that of TGFs, as shown in the TEM images (**Figure 3**a,b). Corresponding statistics of the sheet orientations at different positions further

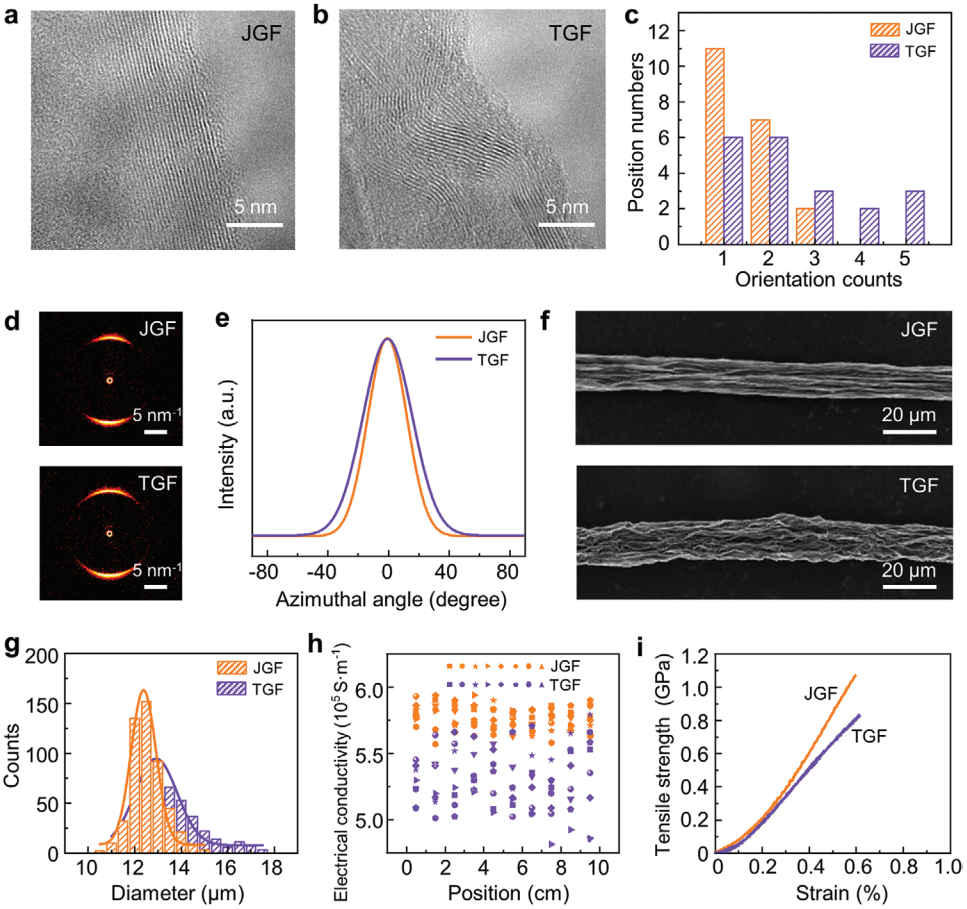


**Figure 3.** Structure and property comparisons between JGFs and TGFs. a,b) Representative TEM images of JGFs (a) and TGFs (b). c) Statistic of the position numbers with the specific number of graphene sheet orientations. *X*-axis represents the orientation count of the graphene sheets and the *Y*-axis represents the statistical number of TEM positions with the specific number of graphene sheet orientations. Twenty TEM images were included in total. d,e) WAXS patterns (d) of JGFs (top) and TGFs (bottom) and the corresponding azimuthal scan profiles (e). f) SEM images of JGFs (top) and TGFs (bottom). g) Diameter statistics of JGFs and TGFs from fifty fiber samples and ten different positions on each fiber. h) Electrical conductivity at different positions of JGFs (orange) and TGFs (violet). Different data markers represent the electrical conductivity along different fiber filaments. i) Representative tensile strength–strain curves of JGFs (orange) and TGFs (violet).

indicate that the graphene sheets in JGFs exhibit more regular alignment than those in TGFs (Figure 3c). Details of the statistical method are illustrated in Figure S9, Supporting Information. Wide-angle X-ray scattering (WAXS) pattern of JGFs presents a higher Herman's orientation factor (JGFs: 0.73, TGFs: 0.61) as well as a narrower full width at half maximum (FWHM) in azimuthal scan profiles (JGFs: 30.5 °, TGFs: 38.8 °) (Figure 3d,e), confirming the better alignment. Meanwhile, scanning electron microscope (SEM) images (Figure 3f) and corresponding diameter statistics (Figure 3g) reveal that JGFs have smaller average diameter and narrower diameter distribution (12.4 ± 0.5 μm), in comparison with TGFs (12.9 ± 0.9 μm). Thus, the JGFs with a reduced structure disorder and smaller average diameter exhibit 11% and 20% enhancement in electrical conductivity and tensile strength, compared with TGFs (Figure 3h,i). Apart from the comparisons between JGFs and TGFs treated under 2000 °C, the JGFs and TGFs treated under different temperature, such as 1500 °C, were also compared, where JGFs-1500 also show superior performances compared with TGFs-1500 (Figure S10, Supporting Information).

To elucidate the role of electric current in improving the alignment of graphene sheet component units in graphene fibers, extensive simulations related to the electric free energy ($G_e$) and electric-current-induced torque ($\tau$) in this system were conducted (see Supporting Information for more calculation details). The schematic in **Figure 4**a presents the conformational change of graphene sheets before and after joule heating, where $\theta$ is the inclined angle between the plane of graphene sheet and the fiber axis. $\theta = 0°$ and 90° represent the states of graphene sheet parallel and vertical to the current flow direction, respectively. The current density distribution around the graphene sheet at inclined angles ranging from 0° to 90° was simulated as in Figure 4b and Figure S11, Supporting Information. Based on the current density distribution, the further calculated results show that $G_e$ has a lowest value when $\theta = 0°$, indicating that the state of graphene sheet parallel to current direction is the most thermodynamically stable (Figure 4c). Kinetically, the current can induce a high torque, which can drive the sheet rotating to the most stable state of $\theta = 0°$ with the minimum torque equals to zero (Figure 4d).

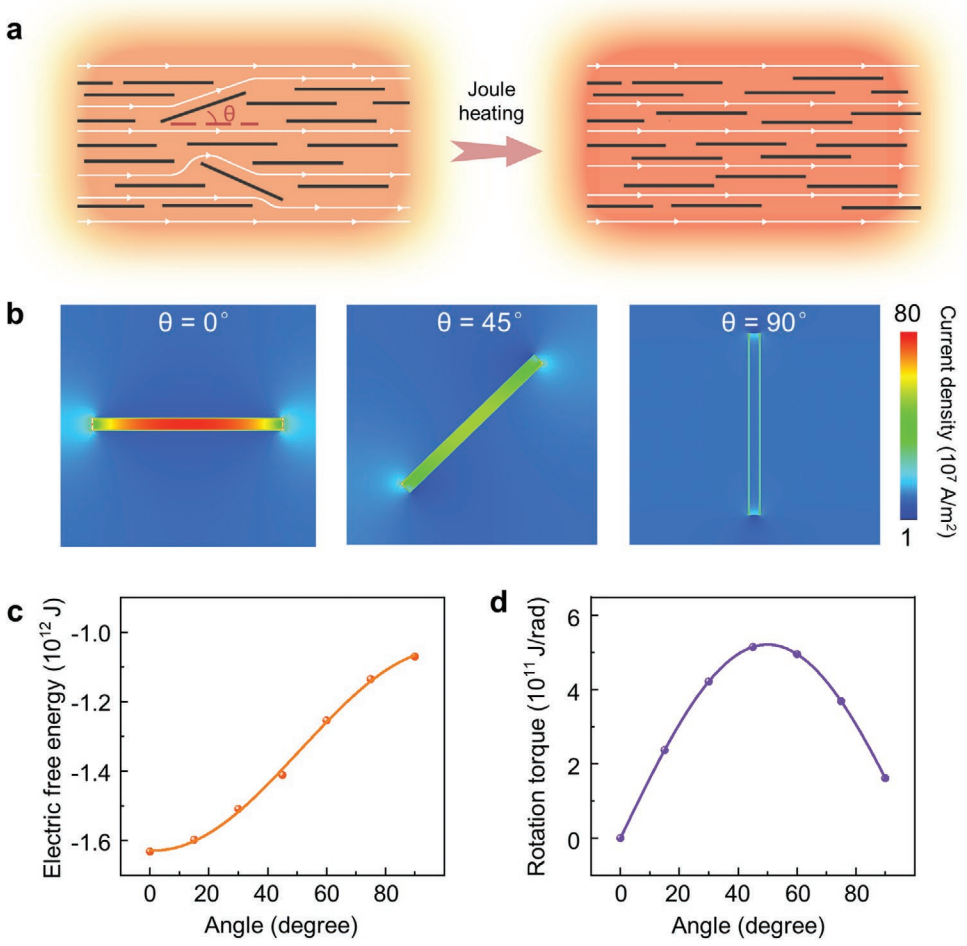


**Figure 4.** Theoretical simulations of the electric current-induced graphene sheets alignment in DJH process. a) Schematic showing the conformational change of the graphene sheets before (left) and after (right) joule heating, where $\theta$ represents the inclined angle between the plane of graphene sheet and the fiber axis. b) Simulated distribution of current density around the graphene sheet with different inclined angles ($\theta = 0°$, 45°, 90°). c,d) Changes of electric free energy (c) and electric-current-induced torque (d) with respect to the sheet inclined angle $\theta$.

## 3. Conclusion

In conclusion, we propose the innovative DJH method enabling the ultrafast and continuous fabrication of graphene fibers. The high-temperature treatment duration of graphene fibers in joule heating can be one order of magnitude shorter than that of previously reported conventional thermal treatments. During joule heating, the electric current flowing through the JGFs can manipulate the conformation of graphene sheet component units to prompt their alignment along the fiber axis, resulting in distinct improvements of Herman's orientation factor, electrical conductivity, and tensile strength with respect to those of TGFs. The DJH method featured with current-inducing effects can be extended to the continuous synthesis of versatile assembled materials, synchronously achieve the conformation control of the component units, and engineer their macroscopic performances.

## 4. Experimental Section

*Pretreatment of GO Fiber*: GO fibers with 100 filaments were purchased from Hangzhou Gaoxi Technology Co. Ltd, which were synthesized according to the previously reported wet spinning procedures.[24,27] The fibers were then chemically reduced in the hydriodic acid solution (30 wt%) overnight at 90 °C. After washing by water and ethanol sequentially, the rGOFs were dried on an oven under the argon atmosphere at 80, 200, and 300 °C, successively.

*Dynamic Joule Heating of rGOFs*: Before joule heating, a bundle of rGOFs with 100 filaments was fixed on the two winding rollers inside a 3-inch quartz tube and system was pumped to a pressure of <1 Pa. The fibers were firstly annealed at the speed of 5 mm $min^{-1}$ under 200 sccm (standard cubic centimeters per min) argon and 10 sccm hydrogen with an input voltage of 55 V and a corresponding current density of $\approx 3.4 \times 10^7$ A $m^2$, with the system pressure of ≈100 Pa. Afterwards, the fibers were switched back to the supplying roller and were then operated from the supplying roller to the receiving roller with an input voltage ranging from 70 to 90 V (corresponding current density ranging from $\approx 0.9 \times 10^8$ to $\approx 1.2 \times 10^8$ A $m^2$ and the temperature ranging from 1500 to 2000 °C) at the same moving speed under 10 sccm hydrogen with the system pressure of ≈5 Pa. The temperature profile of graphene fibers was recorded by an infrared camera (PICONNECTOW-05M).

*Thermally Annealing rGOFs*: A reel of rGOFs was loaded in a graphitization furnace. Then the sample was heated to 1100 °C under the mixture gas of 200 sccm argon and 10 sccm hydrogen at a rate of 1000 °C $h^{-1}$. After a 10-min duration, the fibers were then heated to 2000 °C with the same temperature raising rate, followed by another 10-min annealing. After naturally cooling down to the room temperature in the protection gas of argon and hydrogen, the TGFs were obtained.

*Characterization*: SEM (FEI Quattro S, 20 kV), HR-TEM (FEI Tecnai F20, 200 kV), Raman spectroscopy (Horiba, LabRAM HR-800, 532 nm laser wavelength, 50× objective), energy disperse spectroscopy (EDS) (DigiView/Octane Elect), XPS (Kratos Analytical Axis-Ultra spectrometer, Al K$\alpha$ X-ray source) were applied to characterize the structure, morphology, crystallinity, and components of as-fabricated fiber samples, respectively. SAXS and WAXS measurements were carried out on a Bruker Nanostar instrument, operated at 50 kV and 1 mA. For SAXS characterization, the distance between sample and detector was set as 107 cm with a scanning range of scattering angles from 0.2 to 2.8 degrees ($2\theta$). While in WAXS characterization, the sample was 6 cm away from the detector. Electrical property of graphene fibers was characterized by Keithley 4200A-SCS using a standard four-probe method. Tensile tests were measured on a universal testing machine (Hitachi EZ-LX), while the gauge length and the loading rate were set as 5 mm and 0.5 mm $min^{-1}$, respectively.

## Supporting Information

Supporting Information is available from the Wiley Online Library or from the author.

## Acknowledgements

Y.C., G.C., and C.L. contributed equally to this work. This work was supported by the National Key Basic Research Program of China (973) (No. 2016YFA0200103), the National Natural Science Foundation of China (Nos. 51520105003, 51432002, U1904193), Beijing National Laboratory for Molecular Sciences (BNLMS- CXTD-202001), and Beijing Municipal Science & Technology Commission (Nos. Z201100008720006, Z181100004818001).

## Conflict of Interest

The authors declare no conflict of interest.

## Data Availability Statement

Research data are not shared.

## Keywords

component units, conformation order, electric current aligning, graphene fibers, joule heating

Received: April 14, 2021
Revised: June 1, 2021
Published online: June 23, 2021

[1] W. Bao, A. D. Pickel, Q. Zhang, Y. Chen, Y. Yao, J. Wan, K. Fu, Y. Wang, J. Dai, H. Zhu, D. Drew, M. Fuhrer, C. Dames, L. Hu, *Adv. Mater.* **2016**, *28*, 4684.
[2] Y. Chen, K. Fu, S. Zhu, W. Luo, Y. Wang, Y. Li, E. Hitz, Y. Yao, J. Dai, J. Wan, V. A. Danner, T. Li, L. Hu, *Nano Lett.* **2016**, *16*, 3616.
[3] F. Jiang, Y. Yao, B. Natarajan, C. Yang, T. Gao, H. Xie, Y. Wang, L. Xu, Y. Chen, J. Gilman, L. Cui, L. Hu, *Carbon* **2019**, *144*, 241.
[4] W. A. Algozeeb, P. E. Savas, D. X. Luong, W. Chen, C. Kittrell, M. Bhat, R. Shahsavari, J. M. Tour, *ACS Nano* **2020**, *14*, 15595.
[5] D. X. Luong, K. V. Bets, W. A. Algozeeb, M. G. Stanford, C. Kittrell, W. Chen, R. V. Salvatierra, M. Ren, E. A. McHugh, P. A. Advincula, Z. Wang, M. Bhatt, H. Guo, V. Mancevski, R. Shahsavari, B. I. Yakobson, J. M. Tour, *Nature* **2020**, *577*, 647.
[6] Y. Liu, P. Li, F. Wang, W. Fang, Z. Xu, W. Gao, C. Gao, *Carbon* **2019**, *155*, 462.
[7] C. Wang, W. Ping, Q. Bai, H. Cui, R. Hensleigh, R. Wang, A. H. Brozena, Z. Xu, J. Dai, Y. Pei, C. Zheng, G. Pastel, J. Gao, X. Wang, H. Wang, J.-C. Zhao, B. Yang, X. Zheng, J. Luo, Y. Mo, B. Dunn, L. Hu, *Science* **2020**, *368*, 521.
[8] W. Chen, Z. Wang, K. V. Bets, D. X. Luong, M. Ren, M. G. Stanford, E. A. McHugh, W. A. Algozeeb, H. Guo, G. Gao, B. Deng, J. Chen, J. T. Li, W. T. Carsten, B. I. Yakobson, J. M. Tour, *ACS Nano* **2021**, *15*, 1282.
[9] Y. Yao, Z. Huang, P. Xie, S. D. Lacey, R. J. Jacob, H. Xie, F. Chen, A. Nie, T. Pu, M. Rehwoldt, D. Yu, M. R. Zachariah, C. Wang, R. Shahbazian-Yassar, J. Li, L. Hu, *Science* **2018**, *359*, 1489.

[10] K. L. Grosse, M.-H. Bae, F. Lian, E. Pop, W. P. King, *Nat. Nanotechnol.* **2011**, *6*, 287.
[11] M. G. Stanford, K. V. Bets, D. X. Luong, P. A. Advincula, W. Chen, J. T. Li, Z. Wang, E. A. McHugh, W. A. Algozeeb, B. I. Yakobson, J. M. Tour, *ACS Nano* **2020**, *14*, 13691.
[12] Y. Yao, K. K. Fu, C. Yan, J. Dai, Y. Chen, Y. Wang, B. Zhang, E. Hitz, L. Hu, *ACS Nano* **2016**, *10*, 5272.
[13] R. Qin, *Sci. Rep.* **2017**, *7*, 8449.
[14] L. Yan, X. Zhang, *Steel Res. Int.* **2019**, *91*, 1900465.
[15] X. Zhang, R. Qin, *Mater. Sci. Technol.* **2017**, *33*, 1399.
[16] X. Zhang, R. Qin, *Appl. Phys. Lett.* **2014**, *104*, 114106.
[17] A. Rahnama, R. S. Qin, *Scr. Mater.* **2015**, *96*, 17.
[18] A. S. Mayorov, R. V. Gorbachev, S. V. Morozov, L. Britnell, R. Jalil, L. A. Ponomarenko, P. Blake, K. S. Novoselov, K. Watanabe, T. Taniguchi, A. K. Geim, *Nano Lett.* **2011**, *11*, 2396.
[19] A. A. Balandin, S. Ghosh, W. Bao, I. Calizo, D. Teweldebrhan, F. Miao, C. N. Lau, *Nano Lett.* **2008**, *8*, 902.
[20] C. Lee, X. Wei, J. W. Kysar, J. Hone, *Science* **2008**, *321*, 385.
[21] Y. Cheng, K. Wang, Y. Qi, Z. Liu, *Acta Phys.-Chim. Sin.* **2021**, *37*, 2006046.
[22] T. Xu, Z. Zhang, L. Qu, *Adv. Mater.* **2019**, *32*, 1901979.
[23] Z. Xu, C. Gao, *Nat. Commun.* **2011**, *2*, 571.
[24] Z. Xu, H. Sun, X. Zhao, C. Gao, *Adv. Mater.* **2013**, *25*, 188.
[25] M. Jian, Y. Zhang, Z. Liu, *Acta Phys.-Chim. Sin.* **2021**, *37*, 2007093.
[26] B. Fang, D. Chang, Z. Xu, C. Gao, *Adv. Mater.* **2019**, *32*, 1902664.
[27] Z. Xu, Y. Liu, X. Zhao, L. Peng, H. Sun, Y. Xu, X. Ren, C. Jin, P. Xu, M. Wang, C. Gao, *Adv. Mater.* **2016**, *28*, 6449.
[28] G. Xin, T. Yao, H. Sun, S. M. Scott, D. Shao, G. Wang, J. Lian, *Science* **2015**, *349*, 1083.
[29] G. Xin, W. Zhu, Y. Deng, J. Cheng, L. T. Zhang, A. J. Chung, S. De, J. Lian, *Nat. Nanotechnol.* **2019**, *14*, 168.
[30] C. Xiang, C. C. Young, X. Wang, Z. Yan, C. C. Hwang, G. Cerioti, J. Lin, J. Kono, M. Pasquali, J. M. Tour, *Adv. Mater.* **2013**, *25*, 4592.
[31] T. Ma, H. L. Gao, H. P. Cong, H. B. Yao, L. Wu, Z. Y. Yu, S. M. Chen, S. H. Yu, *Adv. Mater.* **2018**, *30*, 1706435.
[32] B. Zheng, W. Gao, Y. Liu, R. Wang, Z. Li, Z. Xu, C. Gao, *Carbon* **2020**, *158*, 157.
[33] P. Li, Y. Liu, S. Shi, Z. Xu, W. Ma, Z. Wang, S. Liu, C. Gao, *Adv. Funct. Mater.* **2020**, *30*, 2006584.
[34] F. G. Emmerich, *Carbon* **2014**, *79*, 274.
[35] X. Huang, *Materials* **2009**, *2*, 2369.
[36] L. Qiu, X. H. Zheng, J. Zhu, G. P. Su, D. W. Tang, *Carbon* **2013**, *51*, 265.